

# The Frequency Diverse Pulse-Pair algorithm for Doppler velocity estimation

V. VENKATESH<sup>1,2</sup>, L. LI<sup>1</sup>, M. MCLINDEN<sup>1</sup>, M. COON<sup>1</sup>, and G. HEYMSFIELD<sup>1</sup>

<sup>1</sup>NASA Goddard Space Flight Center, Greenbelt, MD

<sup>2</sup>Science Systems and Applications Inc, Lanham, MD,

## 1. Introduction

Space-borne measurements of Doppler velocity, although capable of adding valuable insights on latent heating (et al. (2006)) and microphysics (Wilson et al. (1997)), remain undemonstrated. This is because massive spacecraft speeds along with the use of a non-trivial beamwidth combine to produce large spectrum widths (Amayenc et al. (1993), Kobayashi et al. (2001)). By the Wiener-Khinchine theorem, the Doppler spectrum and the auto-correlation function form a Fourier pair. Consequently, broad Doppler spectra leads to signal decorrelation so rapid that there is little coherence on timescales comparable to PRFs needed to sample the entire troposphere. Techniques to resolve the Doppler-Range ambiguity dilemma offer a possible solution. For example, the Polarization Diverse Pulse-Pair (PDPP) (Pazmany et al. (1999)) transmits a two pulse train with orthogonal polarizations. The idea is that the two-pulse train provides adequate sampling of the Doppler spectrum, while the PRT can be adjusted independently for range coverage. However, finite polarization isolation may overwhelm retrievals close to the surface (Battaglia et al. (2013)). A possible alternative is the use of frequency diversity (in lieu of polarization diversity). If proven practical, this frequency diverse pulse-pair method would potentially provide low-cost Doppler velocity retrievals from space-borne platforms.

## 2. Methodology

### a. Conceptual description of FDPP algorithm

Two pulses at center frequencies  $f_1$  and  $f_2$  are transmitted separated by some lag  $\Delta T$ . While retaining  $\Delta T$ , the order of the pulses is reversed every alternate transmission. From the receive channels at  $f_1$  and  $f_2$ , the pulse-pair phase estimate of the two sequences are individually accumulated and stored as  $\Delta\phi_{order1}$  and  $\Delta\phi_{order2}$ . Finally Doppler velocity is estimated from the sum of the two individual pulse-pair phase estimates (denote as  $\Delta\phi$ ). Note that the use of two closely spaced radar frequencies introduces two primary sources of error. First, a “beat” phase that scales as a function of range is introduced. Nonethe-

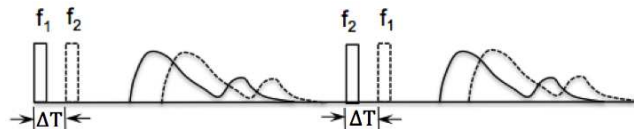


FIG. 1. Illustration of the Frequency Diversity Pulse-Pair (FDPP) concept. Two short pulses - modulated by frequencies  $f_1$  and  $f_2$  are transmitted during the first pulse repetition interval. During the next PRI, the pulses are modulated by frequencies  $f_2$  and  $f_1$  respectively. There are two mechanisms for error cancellation. First, the “beat” phases of the  $f_1$ - $f_2$  and  $f_2$ - $f_1$  pairs cancel out in the expected value sense. Second, since the  $f_1$ - $f_2$  and  $f_2$ - $f_1$  phase estimates are highly anti-correlated, the sum of the two phase estimates has a much smaller variance than the individual phase estimates.

less, this term vanishes when the phases of the  $f_1$ - $f_2$  pair and  $f_2$ - $f_1$  pairs are added. Second, since there is little correlation between the  $f_1$  and  $f_2$  pulses, the variances of the  $f_1$ - $f_2$  phase estimates is large. However, since the  $f_1$ - $f_2$  and  $f_2$ - $f_1$  phase estimates are highly anti-correlated, the sum of the two phase estimates has a much smaller variance.

### b. Mathematical description of FDPP algorithm

Denote the transmitted waveform at frequency  $f_1$  as  $E_{TX,f1}(t)$ . Let  $E_{0,f1}$  be the amplitude of the transmitted signal, the phase of the transmitted signal be  $\Psi_{TX,f1}$  and  $t$  denote time.

$$E_{TX,f1}(t) = E_{0,f1} \cos[2\pi f_1 t + \Psi_{TX,f1}] \quad (1)$$

Denote  $c$  be the speed of light,  $f_{D1}$  be the Doppler shift and  $R$  the range to a point scatterer. Now, the received signal  $E_{RX,f1}$  at time  $t$  can be written as

$$E_{RX,f1}(t) = A_{f1} E_{0,f1} \cos[2\pi(f_1 + f_{D1})(t + \frac{2R}{c}) + \Psi_{TX,f1}] \quad (2)$$

Similarly, the  $TX$  and  $RX$  signals at frequency  $f_2$  and time  $t + \Delta T$  can be written as follows. Note that the range

to the point-scatterer is now  $R + v_r \Delta T$ . Here,  $v_r$  denotes the radial velocity of the point-scatterer.

$$E_{TX,f_2}(t + \Delta T) = E_{0,f_2} \cos[2\pi f_2(t + \Delta T) + \Psi_{TX,f_2}] \quad (3)$$

$$E_{RX,f_2}(t + \Delta T) = A_{f_2} E_{0,f_2} \cos[2\pi(f_2 + f_{D2})(t + \frac{2(R+v_r \Delta T)}{c}) + \Psi_{TX,f_2}]$$

Assume  $A_{f_1} = A_{f_2}$ ,  $E_{0,f_1} = E_{0,f_2}$ ,  $f_1 \gg f_{D1}$  and  $f_2 \gg f_{D2}$ . Denote the echo phase  $\phi_{RX} - \phi_{TX}$  for the frequencies  $f_1$  and  $f_2$  as  $\Phi_{f_1}$  and  $\Phi_{f_2}$  respectively.

$$\Phi_{f_1} = 2\pi f_1(t + \frac{2R}{c}) + \Psi_{TX,f_1} - 2\pi f_1 t - \Psi_{TX,f_1} \quad (4)$$

$$\Phi_{f_1} = 2\pi f_1 \frac{2R}{c} \quad (5)$$

$$\Phi_{f_2} = 2\pi f_2[(t + \Delta T) + \frac{2(R + \Delta T)}{c}] - 2\pi f_2(t + \Delta T) \quad (6)$$

$$\Phi_{f_2} = 2\pi f_2 \frac{2R + 2v_r \Delta T}{c} \quad (7)$$

The frequency-diverse pulse pair algorithm is based on the two quantities  $\Delta\Phi_{order1}$  and  $\Delta\Phi_{order2}$ . Here,  $\Delta\Phi_{order1} = \Phi_{f_2} - \Phi_{f_1}$  and  $\Delta\Phi_{order2} = \Phi_{f_1} - \Phi_{f_2}$ . Denote  $\lambda_1 = c/f_1$ ,  $k_1 = \frac{2\pi}{\lambda_1}$ ,  $\lambda_2 = c/f_2$  and  $k_2 = \frac{2\pi}{\lambda_2}$ .

$$\Delta\Phi_{order1} = 2R_{order1}(k_1 - k_2) + 2k_1 v \Delta T \quad (8)$$

Similarly,

$$\Delta\Phi_{order2} = 2R_{order2}(k_2 - k_1) + 2k_2 v \Delta T \quad (9)$$

Recognizing that  $R_{order2} = R_{order1} + v\tau$ . Here  $\tau$  denotes the pulse repetition time. Denote  $\Delta\Phi = \Delta\Phi_{order1} + \Delta\Phi_{order2}$ .

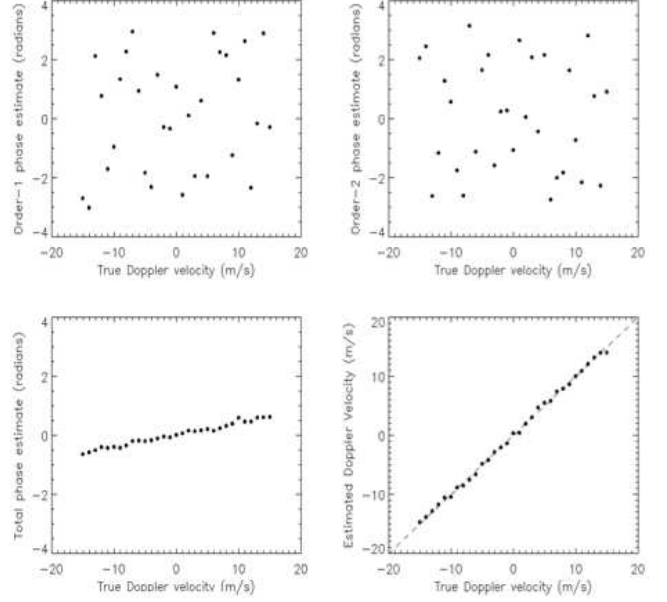
$$\Delta\Phi = 2(k_2 - k_1)v_r\tau + 2(k_1 + k_2)v_r\Delta T \quad (10)$$

$$\Delta\Phi = 2[(k_2 - k_1)\tau + (k_1 + k_2)\Delta T]v_r \quad (11)$$

Since all values other than  $v_r$  are solely system dependent, the radial component of target mean radial velocity  $v_r$  can be obtained from the ensemble-averaged  $\Delta\Phi$ . Let  $\sigma$  denote the variance and  $\rho$  denote the correlation operators respectively.

$$\sigma(\Delta\Phi) = \sigma(\Delta\Phi_{order1}) + \sigma(\Delta\Phi_{order2}) + 2Cov(\Delta\Phi_{order1}, \Delta\Phi_{order2})$$

Now, the covariance term can be conveniently decomposed as



(a)

FIG. 2. Monte-Carlo simulations illustrating the FDPP algorithm concept. Clockwise from top left. (a) Phase estimates from  $f_1$ - $f_2$  pulse-pair ( $\Delta\phi_{order1}$ ). (b) Phase estimates from  $f_2$ - $f_1$  pulse-pair ( $\Delta\phi_{order2}$ ). (c) FDPP Doppler estimates using a scaled version of (d). (d) Sum of Fig. 2a and 2b., after unwrapping.

$$Cov(\Delta\Phi_{order1}, \Delta\Phi_{order2}) = \rho(\Delta\Phi_{order1}, \Delta\Phi_{order2}) \cdot \sqrt{\sigma(\Delta\Phi_{order1}) \cdot \sigma(\Delta\Phi_{order2})}$$

For cases where  $\sigma(\Delta\Phi_{order1}) = \sigma(\Delta\Phi_{order2})$ ,

$$Cov(\Delta\Phi_{order1}, \Delta\Phi_{order2}) = \rho(\Delta\Phi_{order1}, \Delta\Phi_{order2}) \cdot \sigma(\Delta\Phi_{order1})$$

From the above relationships,

$$\sigma(\Delta\Phi) = 2\sigma(\Delta\Phi_{order1}) + 2\rho(\Delta\Phi_{order1}, \Delta\Phi_{order2}) \cdot \sigma(\Delta\Phi_{order1}) \quad (12)$$

Rearranging terms in (12),

$$\sigma(\Delta\Phi) = 2\sigma(\Delta\Phi_{order1})[1 + \rho(\Delta\Phi_{order1}, \Delta\Phi_{order2})] \quad (13)$$

The underlying premise of the frequency-diverse pulse-pair algorithm is that as  $\rho(\Delta\Phi_{order1}, \Delta\Phi_{order2}) \rightarrow -1$ , the variance of the phase composite estimate  $\sigma(\Delta\Phi) \rightarrow 0$ .

### 3. Preliminary Results

In this section, Monte-Carlo simulations are qualitatively compared with data-analysis results (all at W-band). Fig. 2 shows simulations of the FDPP Doppler velocity retrieval process. The basic idea is that a composite phase that is solely Doppler dependent is synthesized from noisy

but highly anti-correlated frequency diverse pulse-pair lag-1 phase estimates. The phase estimate from the sequence in which  $f_1$  leads  $f_2$  is shown in Fig. 2a. After 1 PRT, the sequence of  $f_2$  followed by  $f_1$  yields phase estimates shown in Fig. 2b. The sum of the two frequency diverse pulse-pair estimates is shown in Fig. 2c. Fig. 2d shows a scaled version of Fig.2c, where the composite phase is scaled to the Doppler Nyquist interval.

Fig. 3 shows the FDPP algorithm Doppler retrieval accuracy for a W-band radar as a function of various design parameters. The simulation methodology employed herein is similar to that in Venkatesh and Frasier (2013). Typically, 1000 Monte-Carlo tries were employed to generate the simulation statistics. The relevant parameters shown in the corresponding figures. From Fig. 3a, we see that the improvement in Doppler retrieval error is small for antenna sizes beyond 5 m. Consequently, we deem a 5m antenna size optimal at W-band. A similar reasoning deems a 6.5 kHz and 2 Km along-track integration length optimal. In Fig. 3c, the increasing errors on the right side are a direct consequence of decreasing correlation between the  $f_1$ - $f_2$  and  $f_1$ - $f_2$  pair phase estimates. The increasing errors on the left hand side are due to sensitivity to thermal noise. As expected, this is exacerbated at shorter lags and decreasing  $SNR$ .

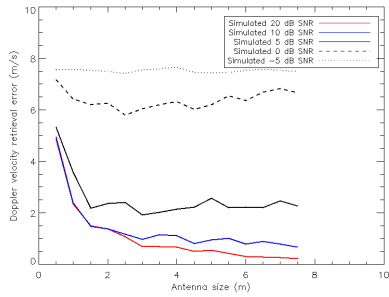
Fig. 4 shows data analysis results from a frequency diverse pulse-pair implementation on the NASA GSFC Cloud Radar System (CRS) (Li et al. (2004)). For the purpose of this preliminary demonstration, the radar was slowly slewed across stationary ground clutter targets. Conventional single frequency pulse-pair Doppler estimates were employed as truth. The good agreement of the FDPP Doppler estimates with the conventional pulse-pair estimates validates the FDPP concept to first order on hard-targets.

#### 4. Summary

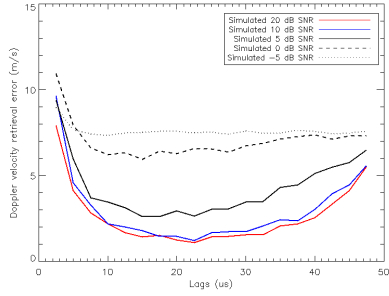
- i. Spaceborne weather radar Doppler measurement is challenging due to wide Doppler spectra. Essentially, this exacerbates the Doppler-range dilemma.
- ii. An innovative Frequency Diversity Pulse-Pair (FDPP) technique is proposed and studied for extending the Doppler Nyquist range, and therefore to enable Doppler unfolding and Doppler retrieval from fast moving platform.
- iii. With modern digital waveform generation, digital receiver and solid-state power amplifier technologies, FDPP can be implemented without additional hardware.
- iv. Compared to Polarization Diversity, FDPP provides better channel isolation, therefore better mitigates contamination from strong targets, such as the ground or ocean surface.
- v. The FDPP algorithm was implemented on the NASA GSFC Cloud Radar System (CRS) and backscattered signal from hard-targets were used for preliminary evaluation. Data collection and analysis efforts on weather targets from an airborne platform are planned during an upcoming field campaign in Winter (OLYMPLEX).
- vi. The FDPP technique is also promising for other applications such as military aircraft, missile detection and air traffic control.

#### REFERENCES

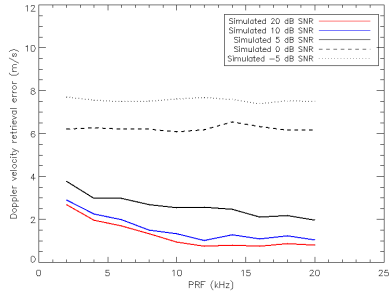
- Amayenc, P., J. Testud, and M. Marzoug, 1993: Proposal for a spaceborne dual-beam rain radar with doppler capability. *J. Atmos. Oceanic. Tech.*, **10**, 262–276.
- Battaglia, A., S. Tanelli, and P. Kollias, 2013: Polarization diversity for millimeter wave spaceborne doppler radars: An answer for observing deep convection ? *J. Atmos. Oceanic. Tech.*, **30**, 2768–2787.
- et al., W.-K. T., 2006: Retrieval of latent heating from trmm measurements. *Bull. Amer. Meteor. Soc.*, **87**, 1555–1572.
- Kobayashi, S., H. Kumagai, and H. Kuroiwa, 2001: A proposal of pulse-pair doppler operation on a spaceborne cloud-profiling radar in the w-band. *J. Atmos. Oceanic. Tech.*, **19**, 1294–1306.
- Li, L., G. Heymsfield, P. Racette, L. Tian, and E. Zenker, 2004: A 94 ghz cloud radar system on a nasa high-altitude er-2 aircraft. *J. Atmos. Oceanic. Tech.*, **21**, 1378–1388.
- Pazmany, A., J. C. Galloway, J. Mead, I. Popstefanija, R. McIntosh, and H. Bluestein, 1999: Polarization diversity pulse-pair technique for millimeter-wave doppler radar measurements of severe storm measurements. *J. Atmos. Oceanic. Tech.*, **16**, 1900–1911.
- Venkatesh, V. and S. Frasier, 2013: Simulation of spaced antenna wind retrieval performance on an x-band active phased array weather radar. *J. Atmos. Oceanic. Tech.*, **30**, 1447–1459.
- Wilson, D., A. Illingworth, and T. Blackman, 1997: Differential doppler velocity: A radar parameter for characterizing hydrometeor size distributions. *Journal of Applied Meteorology*, **36**, 649–663.



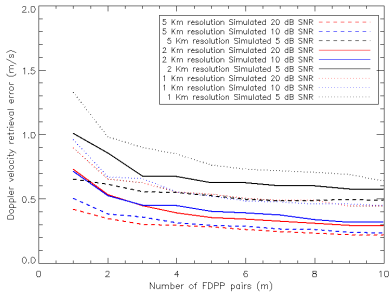
(a)



(b)



(c)



(d)

FIG. 3. Monte-Carlo simulations of the FDPP algorithm error space. Clockwise from top left. (a) FDPP Doppler retrieval error as a function of antenna size. (b) FDPP Doppler retrieval error as a function of Pulse Repetition Frequency. (c) FDPP Doppler retrieval accuracy as a function of number of simultaneously transmitted/received FDPP pairs for 1 Km, 2 Km and 5 Km along-track integration lengths. (d) FDPP Doppler retrieval error as a function of time-lag.

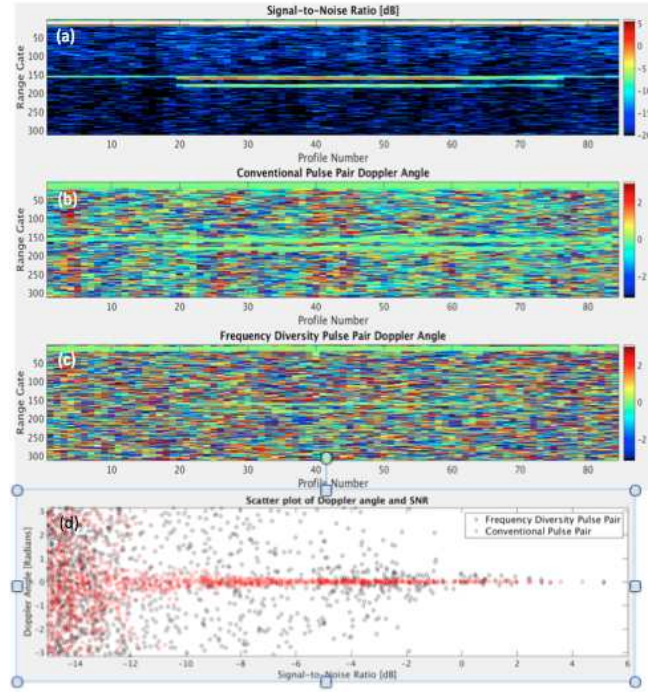


FIG. 4. Roof top test using the NASA GSFC W-band radar with a FDPP pulse-pair time-lag of 30 micro-seconds and 5 kHz PRF. Top to Bottom - (a) Backscattering power to receiver noise ratio (signals at zero-range are Tx leakages), (b) Doppler phase estimated using conventional pulse-pair algorithm. (c) Doppler phase estimated using FDPP algorithm. (d) Scatter plot shows that the FDPP algorithm agrees with with conventional pulse-pair results for high SNR targets. (e) The NASA GSFC Cloud Radar System (CRS). Radar parameters follow. Frequency : 94 GHz, Transmitter type : Solid State Power Amplifier (SSPA), Tx power : 30 Watts, Antenna Beamwidth : 0.6 degrees by 0.8 degrees, Pulsewidth : 2 micro-seconds, PRF : Staggered 4/5 kHz, FDPP time-lag : 30 micro-seconds.